

Exploring Dephasing of a Solid-State Quantum Emitter via Time- and Temperature-Dependent Hong-Ou-Mandel Experiments

A. Thoma,¹ P. Schnauber,¹ M. Gschrey,¹ M. Seifried,¹ J. Wolters,¹ J.-H. Schulze,¹ A. Strittmatter,¹
S. Rodt,¹ A. Carmele,² A. Knorr,² T. Heindel,^{1,*} and S. Reitzenstein¹

¹Institut für Festkörperphysik, Technische Universität Berlin, Hardenbergstraße 36, 10623 Berlin, Germany

²Institut für Theoretische Physik, Technische Universität Berlin, Hardenbergstraße 36, 10623 Berlin, Germany

(Received 22 July 2015; published 19 January 2016)

We probe the indistinguishability of photons emitted by a semiconductor quantum dot (QD) via time- and temperature-dependent two-photon interference (TPI) experiments. An increase in temporal separation between consecutive photon emission events reveals a decrease in TPI visibility on a nanosecond time scale, theoretically described by a non-Markovian noise process in agreement with fluctuating charge traps in the QD's vicinity. Phonon-induced pure dephasing results in a decrease in TPI visibility from $(96 \pm 4)\%$ at 10 K to a vanishing visibility at 40 K. In contrast to Michelson-type measurements, our experiments provide direct access to the time-dependent coherence of a quantum emitter on a nanosecond time scale.

DOI: 10.1103/PhysRevLett.116.033601

Bright nonclassical light sources emitting single indistinguishable photons on demand constitute key building blocks towards the realization of advanced quantum communication networks [1–5]. In recent years, single self-assembled quantum dots (QDs) integrated into photonic microstructures have turned out to be very promising candidates for realizing such quantum-light sources [6–10], and enabled, for instance, a record-high photon indistinguishability of 99.5 % using self-organized InAs QDs under strict-resonant excitation [11]. Further advancement of quantum optical experiments and applications of QDs beyond proof-of-principle demonstrations, however, will certainly rely on deterministic device technologies and should be compatible with scalable fabrication platforms. Furthermore, profound knowledge of the two-photon interference (TPI) is crucial for an optimization of novel concepts and devices in the field of advanced quantum information technology. In this respect, previous experiments utilizing QDs showed that dephasing crucially influences the indistinguishability of the photons emitted by the QD states, while a detailed understanding of the involved processes has been elusive [12–15]. In fact, these experiments revealed the difficulty of giving an adequate measure of the coherence time T_2 of QDs. They even triggered a debate of how to correctly interpret T_2 obtained via Michelson interferometry, which typically gives a lower bound for the visibilities observed experimentally in Hong-Ou-Mandel (HOM)-type [16] TPI experiments [12,15,17]. A commonly accepted—although not proven—explanation for this apparent discrepancy is the presence of spectral diffusion on a time scale which is long compared to the excitation-pulse separation of a few nanoseconds typically used in HOM studies, but much shorter than the integration times of Michelson experiments. In this context, more direct experimental access to the time dependent dephasing processes and their theoretical description is highly beneficial [18,19].

In this work, we map the coherence of a solid-state quantum emitter in the presence of pure dephasing by means of HOM-type TPI experiments. The time scale of the involved decoherence processes is precisely probed using an excitation sequence at which the temporal pulse-separation δt is varied. Additionally, temperature-dependent measurements allow us to independently probe the impact of phonon-induced pure dephasing on the indistinguishability of photons.

The quantum emitter studied in our experiments is a single InGaAs QD grown by metal-organic chemical vapor deposition (MOCVD) which is deterministically integrated within a monolithic microlens [20,21] (cf. Fig. 1, see also Supplemental Material [22] for details). The quantum optical properties of photons emitted by the deterministic QD microlens are studied via low-temperature microphotoluminescence spectroscopy in combination with HOM-type TPI experiments [cf. Fig. 1(b), see Supplemental Material [22] for experimental details]. A mode-locked Ti:sapphire laser operating in picosecond

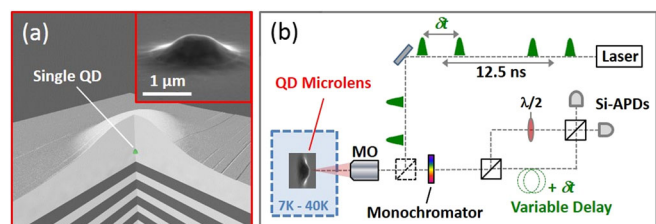


FIG. 1. (a) Schematic view of the cross section of a monolithic microlens with a single deterministically integrated QD. Inset: Scanning electron microscopy image of a fully processed microlens. (b) Experimental setup: Hong-Ou-Mandel-type two-photon interference experiments are utilized to probe the indistinguishability of consecutively emitted photons with variable pulse separation δt (MO: microscope objective, APD: avalanche photodiode).

mode is used to excite the QD at a repetition rate of 80 MHz. The periodic excitation pulses are converted into a sequence of double-pulses with variable pulse-separation δt . This excitation scheme in combination with a HOM-type asymmetric Mach-Zehnder interferometer enables us to probe the TPI visibility of two photons emitted by the QD as a function of the time elapsed between consecutive emission events.

A typical microphotoluminescence (μ PL) spectrum of a deterministic QD microlens chosen for our experiments is depicted in Fig. 2, where the horizontally linearly polarized emission was selected using polarization optics. The QD is excited pulsed ($\delta t = 12.5$ ns) quasiresonantly in its p shell at a wavelength of 909 nm. The assignment of the charge neutral exciton (X^0) and biexciton (XX^0) states as well as the charged trion states (X^+ , X^-), was carried out via polarization and power dependent measurements as described, e.g., in Ref. [32]. For further investigations we first spectrally selected the emission of the X^0 state (cf. markers in Fig. 2). The inset of Fig. 2 shows the corresponding raw measurement data of the second-order photon-autocorrelation $g_{\text{HBT}}^{(2)}(\tau)$.

In contrast to $g_{\text{HBT}}^{(2)}(0)$, the photon indistinguishability, being the crucial parameter for advanced quantum communication scenarios, is particularly sensitive to dephasing processes. The dephasing rate of a quantum emitter is described by its coherence time T_2 and the radiative lifetime $T_1 = \Gamma^{-1}$ via $T_2^{-1} = (2T_1)^{-1} + (T_2^*)^{-1}$ [33], where $(T_2^*)^{-1} = \Gamma' + \gamma$ describes pure dephasing due to spectral diffusion (Γ') and phonon interaction (γ). In the following we gain experimental access to both types of pure dephasing independently by means of time- and temperature-dependent TPI experiments.

First, we use a pulse sequence with 12.5 ns pulse-separation. Figure 3(a) displays the obtained coincidence histogram of the two-photon detection events at the two outputs of the HOM setup. In the case of copolarized photons (solid blue curve), quantum-mechanical TPI manifests in a strongly reduced number of coincidences at $\tau = 0$, if compared to the measurement in the crosspolarized

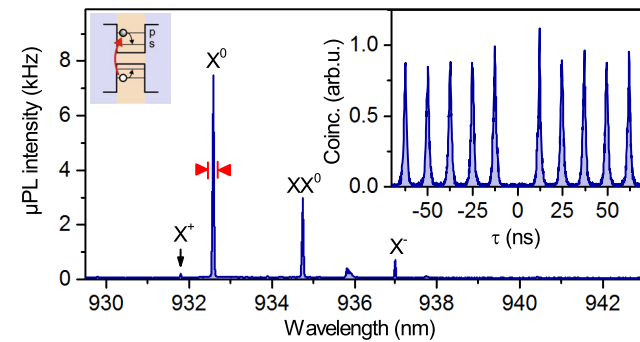


FIG. 2. μ PL spectrum of a deterministic QD microlens under p -shell excitation ($T = 7$ K). Inset: Second-order photon-autocorrelation measurement on the X^0 emission, demonstrating close to ideal single-photon emission.

configuration (dashed grey curve). To quantitatively extract the visibility of TPI, we fitted Lorentzian profiles to the experimental data in the copolarized configuration and evaluated the relative peak areas according to Ref. [7] (cf. Supplemental Material [22]). Under these excitation conditions, we extract a moderate visibility of $V_{12.5 \text{ ns}} = (53 \pm 8)\%$. A possible explanation for the finite wave packet overlap is an inhomogeneous spectral broadening of the QD transition due to spectral diffusion, leading to a pure dephasing rate Γ' as mentioned above. Such processes are typically characterized by a certain time scale depending on specific material properties and growth conditions [7,17,34–38].

To perform a time-dependent analysis of Γ' and the underlying dephasing mechanism, we gradually reduce the pulse separation δt [cf. Fig. 1(b)], while the respective delay inside the HOM interferometer is precisely matched to assure proper interference of consecutively emitted single photons. The resulting coincidence histograms for pulse separations δt of 8.0, 4.0, and 2.0 ns are presented in Figs. 3(b) to 3(d). The complex coincidence-pulse pattern specific to each δt results from overlapping five-peak structures repeating every 12.5 ns [39] (see Supplemental Material [22] for details). Figure 4(a) summarizes the obtained raw TPI visibilities as a function of the pulse separation δt for the neutral exciton X^0 . At low δt a plateau-like behavior is observed, at which the visibility remains almost constant with values of $V_{2.0 \text{ ns}} = (94 \pm 6)\%$ and $V_{4.0 \text{ ns}} = (88 \pm 4)\%$. For pulse separations larger than 4 ns, a distinct decrease in visibility is observed from

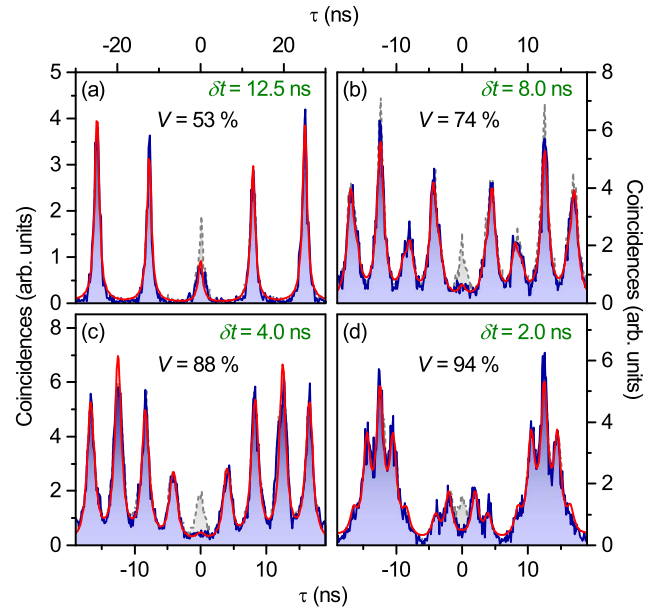


FIG. 3. (a)–(d) Two-photon interference histograms measured using a two-pulse excitation sequence with variable pulse separation δt ($T = 7$ K). Data corresponding to copolarized (crosspolarized) measurement configuration are displayed by solid blue (dashed grey) curves, together with a fit to the data (solid red lines) explained in the main text.

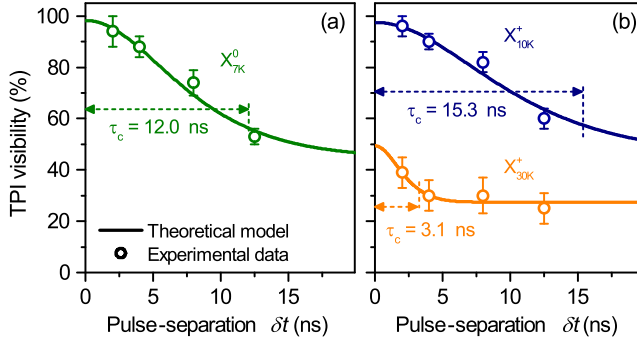


FIG. 4. Two-photon interference visibilities of consecutively emitted single photons versus the time δt elapsed between the emission processes. Experimental data for (a) the X^0 state and (b) the X^+ state are quantitatively described by a theoretical model assuming a non-Markovian noise correlation leading to spectral diffusion on a nanosecond time scale [see Eq. (3)]. A characteristic temperature-dependent correlation time τ_c is observed.

$V_{8.0 \text{ ns}} = (74 \pm 5)\%$ to $V_{12.5 \text{ ns}} = (53 \pm 3)\%$. The significant decrease in TPI visibility at pulse separations larger than 8.0 ns indicates the time scale of spectral diffusion. The time-dependent analysis of Γ' has additionally been carried out for the charged exciton state X^+ of the same QD at 10 K and 30 K [cf. Fig. 4(b)]. We observe again a characteristic correlation time, which decreases at higher temperatures.

In order to gain deeper insight in the underlying dephasing mechanisms, we model the system with a Hamiltonian (see Supplemental Material [22]), where we approximated the QD as a two-level system with transition energy ω_e . To include dephasing, we employ the workhorse of the phenomenological dephasing description by including a general stochastic force $F(t) = P(t) + D(t)$ with a phonon-induced dephasing (δ -correlated white noise) $P(t)$ and a spectral diffusion $D(t)$ component (colored noise), both shifting the transition energy of the QD. The specific noise correlations depend on the coupling mechanism between the QD and its environment. For example, in the case of spectral diffusion, random electric fields due to charge fluctuations induce dephasing [36,40], as discussed later on. Given that the classical (pump) field excites the QD fast enough to prevent multiple photon emission processes, we calculate via the Wigner-Weisskopf method the wave function after the two-pulse sequence:

$$|\Psi(t)\rangle = \int_0^t dt_1 \int_{\delta t}^t dt_2 e^{i(\omega_e + i\Gamma)(t_1 + t_2) - i\phi_{\delta t}(t_2) - i\phi_0(t_1)} \times E_2(t_2) E_1(t_1) |\text{vac}\rangle. \quad (1)$$

This wave function includes the two-photon wave packages $E_n(t_n)$ and the time-integrated stochastic forces defined as $\phi_i^X(t) := \int_t^T dt' X_i(t')$, where $i = 0$ in the case that the photon was emitted during the first sequence or $i = \delta t$ for photon emission processes due to the second pulse and $X(t)$ denoting the noise. Considering the interference at the

beam splitter by unitary transformations on the incident electric fields allows us to calculate the two-photon correlation $\langle E_A^{(-)}(t) E_B^{(-)}(t + \tau) E_B^{(+)}(t + \tau) E_A^{(+)}(t) \rangle$ measured in the experiment at detector A and B . To evaluate the stochastic forces, we need to average via a Gaussian random number distribution $\langle\langle \dots \rangle\rangle$. The $\langle\langle \dots \rangle\rangle$ denotes statistical averaging in terms of a Gaussian random variable, where all higher moments can be expressed by the second-order correlation [41]. Here, we employ the simplest possible model described as a Markovian process δ -correlated in time, i.e., as white noise. It is highly temperature dependent and limits the absolute value of the indistinguishability, independent from the temporal distance of the excitation pulses δt . In contrast to the phonon-induced dephasing, the spectral diffusion reveals a strong dependence on the pulse distance, as seen in Fig. 4. We include this dependence as a finite memory effect with specific correlation time τ_c :

$$\begin{aligned} \langle\langle \phi_{t_1}^D(t_2) \phi_{t_3}^D(t_4) \rangle\rangle &= \int_{t_1}^{t_2} dt \int_{t_3}^{t_4} dt' \langle D(t) D(t') \rangle \\ &= \Gamma'_0 e^{-[(t_1 - t_3)^2 / \tau_c^2]} (\min[t_2, t_4] - \max[t_1, t_3]), \end{aligned} \quad (2)$$

where Γ'_0 describes the maximal amount of pure dephasing induced by spectral diffusion. These kinds of noise correlations stem from a non-Markovian low-frequency noise [40,42,43] and show plateau-like behavior for temporal pulse distances sufficiently short in comparison to the memory depth. Thus, if $\delta t \ll \tau_c$, the effect of spectral diffusion becomes negligible and phonon-induced dephasing limits the absolute value of the visibility. Using these correlations, assuming a balanced beam splitter ($\mathcal{R} = \mathcal{T} = 1/2$) and normalizing the two-photon correlation we derive the following formula, which explicitly depends on the pulse-separation δt :

$$V(\delta t, \tau_c, T) = \frac{\Gamma}{\Gamma'_0 (1 - e^{-(\delta t/\tau_c)^2}) + \gamma(T) + \Gamma}. \quad (3)$$

Here, $\Gamma' := \Gamma'_0 (1 - e^{-(\delta t/\tau_c)^2})$ corresponds to the δt -dependent pure dephasing due to spectral diffusion. In case of vanishing phonon-induced dephasing and spectral diffusion, the TPI visibility is 1; i.e., the photons are Fourier-transform limited and coalesce at the beam splitter into a perfect coherent two-photon state. For low temperatures, the phonon-induced dephasing is small and the spectral diffusion with a finite memory depth dictates the functional form of the visibility for different pulse distances.

Applying the model derived in Eq. (3) to the experimental data of Fig. 4, by fixing Γ (measured independently via time-resolved measurements) and assuming $\gamma_{7 \text{ K}, 10 \text{ K}} = 0$ (cf. next paragraph), we deduce the correlation times τ_c listed in Table I. The time scale at which the noise is correlated appears to be close to the

TABLE I. Correlation times τ_c obtained by fitting Eq. (3) to the experimental data of Fig. 4, fixing $\gamma_{7\text{ K},10\text{ K}} = 0$ and Γ, T_2^∞ values have been calculated from the parameters Γ, Γ'_0 and γ .

Γ (GHz)	Γ'_0 (GHz)	γ (GHz)	τ_c (ns)	T_2^∞ (ps)
$X_{7\text{ K}}^0$	0.85	1.02 ± 0.06	0	12.0 ± 1.9
$X_{10\text{ K}}^+$	0.91	1.03 ± 0.04	0	15.3 ± 2.5
$X_{30\text{ K}}^+$	0.96	1.55 ± 0.78	0.29 ± 1.1	3.1 ± 1.9

fundamental period of the Ti:sapphire laser for $X_{7\text{ K}}^0$ and $X_{10\text{ K}}^+$, whereas an increase in temperature to 30 K shortens the correlation time of X^+ drastically (cf. Table I). Interestingly, the coherence times T_2^∞ inferred from our model in the limit $\delta t \rightarrow \infty$ (see Table I), significantly exceed the values of $T_2 = (291 \pm 6)$ ps for $X_{7\text{ K}}^0$ and $T_2 = (167 \pm 3)$ ps for $X_{30\text{ K}}^+$ obtained via measurements using a Michelson-interferometer (see Supplemental Material [22]). A physical origin of the plateau-like behavior of $V(\delta t)$ and the associated non-Markovian decoherence processes are random flips of bistable fluctuators in the vicinity of the QD [42]. Possible candidates for such fluctuators in solid state devices are charge traps or structural dynamic defects [40]. Further evidence for the presence of charge fluctuations is given by the observation of trion states X^+ and X^- under quasiresonant excitation of the QD (cf. Fig. 2). To reduce the associated electric field noise, weak optical excitation above the bandgap [14] or a static electric field via gates [19] can be applied.

To justify the assumption $\gamma_{7\text{ K},10\text{ K}} = 0$ and to investigate the influence of phonons on the photon indistinguishability in more detail, we performed complementary temperature dependent TPI experiments. For this purpose, the emission of the trion state X^+ was selected under quasiresonant excitation and coupled to the HOM interferometer. The pulse separation was fixed to $\delta t = 2.0$ ns, while the temperature T was varied. Figures 5(a) to 5(c) exemplarily display TPI coincidence histograms for temperatures T of 10, 25, and 35 K in a copolarized measurement configuration. A gradual increase in coincidences at $\tau = 0$ is observed, indicating a reduced photon indistinguishability. The obtained TPI visibilities extracted from the experimental data for temperatures ranging from 10 to 40 K are depicted in Fig. 5(d). At low temperature, we observe close to ideal photon indistinguishability with $V_{10\text{ K}} = (96 \pm 4)\%$. Increasing T results in a distinct decrease of the TPI visibility. Finally, at a temperature of 40 K, V approaches zero within the standard error of our measurement. The observed temperature dependence is further modeled theoretically (red solid line). For this purpose we employed a Markovian approximation for the phonon-induced pure dephasing processes, where the dephasing is proportional to the square of the phonon number [44] (see Supplemental Material [22] for details). The model qualitatively describes our experimental observation. Hence, we conclude that the impact of γ in Eq. (3) is indeed almost negligible at low

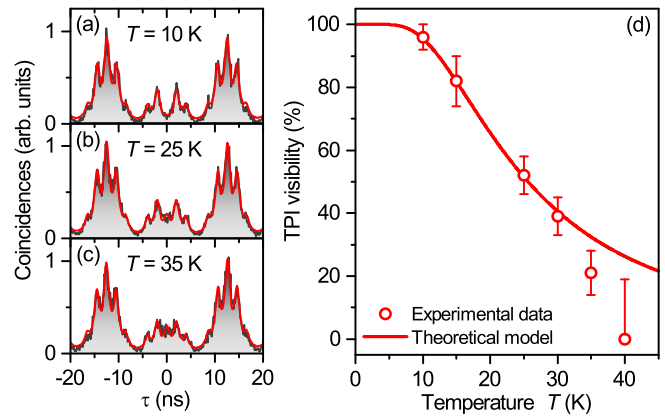


FIG. 5. Impact of the temperature on the two-photon interference (TPI) visibility ($\delta t = 2$ ns). (a)–(c) TPI histograms for copolarized configuration at 10, 25, and 35 K and corresponding fits (red solid curves). (d) Experimentally obtained TPI visibilities for various temperatures. We achieve qualitative agreement with a theoretical model assuming dephasing proportional to the phonon number (see Supplemental Material [22]).

temperatures ($T \leq 10$ K), but has severe impact at elevated temperatures. For temperatures above 30 K, in- and out-scattering with wetting layer carriers also needs to be included, which explains the slight deviation between experiment and theory in this temperature range.

In summary, we presented a method to directly access the time-dependent coherence of a single quantum emitter via HOM-type TPI experiments. We explored the photon indistinguishability as a function of the time δt elapsed between consecutive photon emission events and for different temperatures. We observe TPI visibilities close to unity [$V_{10\text{ K}} = (96 \pm 4)\%$] for MOCVD-grown QDs under p -shell excitation at $\delta t = 2.0$ ns. Increasing δt results in a decrease in visibility on a nanosecond time scale. Our theoretical analysis shows that such behavior can be explained by a non-Markovian dephasing process, which is attributed to spectral diffusion caused by fluctuating charge traps. We independently study the impact of phonon-induced pure dephasing on the photon indistinguishability. Our findings have important implications with respect to the quantum interference of photons emitted by remote emitters [15,45–47] and single-photon multiplexing schemes [48].

We gratefully acknowledge expert sample preparation by R. Schmidt, and thank C. Schneider and C. Matthiesen for stimulating discussions. This work was financially supported by the German Research Foundation (DFG) within the Collaborative Research Center SFB 787 “Semiconductor Nanophotonics: Materials, Models, Devices” and the German Federal Ministry of Education and Research (BMBF) through the VIP-project QSOURCE (Grant No. 03V0630). A. C. gratefully acknowledges support from the SFB 910: “Control of self-organizing nonlinear systems”.

*tobias.heindel@tu-berlin.de

- [1] E. Knill, R. Laflamme, and G. J. Milburn, *Nature (London)* **409**, 46 (2001).
- [2] A. Kiraz, M. Atatüre, and A. Imamoğlu, *Phys. Rev. A* **69**, 032305 (2004).
- [3] P. Kok, W. J. Munro, K. Nemoto, T. C. Ralph, J. P. Dowling, and G. J. Milburn, *Rev. Mod. Phys.* **79**, 135 (2007).
- [4] N. Gisin and R. Thew, *Nat. Photonics* **1**, 165 (2007).
- [5] H. J. Kimble, *Nature (London)* **453**, 1023 (2008).
- [6] P. Michler, A. Kiraz, C. Becher, W. V. Schoenfeld, P. M. Petroff, L. Zhang, E. Hu, and A. Imamoğlu, *Science* **290**, 2282 (2000).
- [7] C. Santori, D. Fattal, J. Vučković, G. S. Solomon, and Y. Yamamoto, *Nature (London)* **419**, 594 (2002).
- [8] R. B. Patel, A. J. Bennett, K. Cooper, P. Atkinson, C. A. Nicoll, D. A. Ritchie, and A. J. Shields, *Phys. Rev. Lett.* **100**, 207405 (2008).
- [9] S. Ates, S. M. Ulrich, A. Ulhaq, S. Reitzenstein, A. Löfller, S. Höfling, A. Forchel, and P. Michler, *Nat. Photonics* **3**, 724 (2009).
- [10] K. Müller, A. Rundquist, K. A. Fischer, T. Sarmiento, K. G. Lagoudakis, Y. A. Kelaita, C. Sánchez Muñoz, E. del Valle, F. P. Laussy, and J. Vučković, *Phys. Rev. Lett.* **114**, 233601 (2015).
- [11] Y.-J. Wei, Y.-M. He, M.-C. Chen, Y.-N. Hu, Y. He, D. Wu, C. Schneider, M. Kamp, S. Höfling, C.-Y. Lu, and J.-W. Pan, *Nano Lett.* **14**, 6515 (2014).
- [12] C. Santori, D. Fattal, J. Vučković, G. S. Solomon, and Y. Yamamoto, *New J. Phys.* **6**, 89 (2004).
- [13] S. Varoutsis, S. Laurent, P. Kramper, A. Lemaître, I. Sagnes, I. Robert-Philip, and I. Abram, *Phys. Rev. B* **72**, 041303 (2005).
- [14] O. Gazzano, S. M. de Vasconcellos, C. Arnold, A. Nowak, E. Galopin, I. Sagnes, L. Lanco, A. Lemaître, and P. Senellart, *Nat. Commun.* **4**, 1425 (2013).
- [15] P. Gold, A. Thoma, S. Maier, S. Reitzenstein, C. Schneider, S. Höfling, and M. Kamp, *Phys. Rev. B* **89**, 035313 (2014).
- [16] C. K. Hong, Z. Y. Ou, and L. Mandel, *Phys. Rev. Lett.* **59**, 2044 (1987).
- [17] A. J. Bennett, D. C. Unitt, A. J. Shields, P. Atkinson, and D. A. Ritchie, *Opt. Express* **13**, 7772 (2005).
- [18] J. Wolters, N. Sadzak, A. W. Schell, T. Schröder, and O. Benson, *Phys. Rev. Lett.* **110**, 027401 (2013).
- [19] M. J. Stanley, C. Matthiesen, J. Hansom, C. Le Gall, C. H. H. Schulte, E. Clarke, and M. Atatüre, *Phys. Rev. B* **90**, 195305 (2014).
- [20] M. Gschrey, F. Gericke, A. Schüßler, R. Schmidt, J.-H. Schulze, T. Heindel, S. Rodt, A. Strittmatter, and S. Reitzenstein, *Appl. Phys. Lett.* **102**, 251113 (2013).
- [21] M. Gschrey, A. Thoma, P. Schnauber, M. Seifried, R. Schmidt, B. Wohlfeil, L. Krüger, J. H. Schulze, T. Heindel, S. Burger, F. Schmidt, A. Strittmatter, S. Rodt, and S. Reitzenstein, *Nat. Commun.* **6**, 7662 (2015).
- [22] See Supplemental Material at <http://link.aps.org/supplemental/10.1103/PhysRevLett.116.033601> for sample growth and processing, details on the experimental setup, the evaluation of the TPI visibility, measurements using a Michelson-interferometer, and the detailed derivation of our theoretical model, which includes Refs. [23–31].
- [23] A. Schlehahn, M. Gaafar, M. Vaupel, M. Gschrey, P. Schnauber, J.-H. Schulze, S. Rodt, A. Strittmatter, W. Stolz, A. Rahimi-Iman, T. Heindel, M. Koch, and S. Reitzenstein, *Appl. Phys. Lett.* **107**, 041105 (2015).
- [24] P. Borri, W. Langbein, S. Schneider, U. Woggon, R. L. Sellin, D. Ouyang, and D. Bimberg, *Phys. Rev. Lett.* **87**, 157401 (2001).
- [25] J. Förstner, C. Weber, J. Danckwerts, and A. Knorr, *Phys. Status Solidi (b)* **238**, 419 (2003).
- [26] E. A. Muljarov and R. Zimmermann, *Phys. Rev. Lett.* **93**, 237401 (2004).
- [27] P. Kaer, N. Gregersen, and J. Mork, *New J. Phys.* **15**, 035027 (2013).
- [28] P. Kaer, P. Lodahl, A.-P. Jauho, and J. Mork, *Phys. Rev. B* **87**, 081308 (2013).
- [29] E. Stock, M.-R. Dachner, T. Warming, A. Schliwa, A. Lochmann, A. Hoffmann, A. I. Toropov, A. K. Bakarov, I. A. Derebezon, M. Richter, V. A. Haisler, A. Knorr, and D. Bimberg, *Phys. Rev. B* **83**, 041304 (2011).
- [30] A. Vagov, M. D. Croitoru, M. Glässl, V. M. Axt, and T. Kuhn, *Phys. Rev. B* **83**, 094303 (2011).
- [31] C. Santori, D. Fattal, K.-M. C. Fu, P. E. Barclay, and R. G. Beausoleil, *New J. Phys.* **11**, 123009 (2009).
- [32] A. Schlehahn, L. Krüger, M. Gschrey, J.-H. Schulze, S. Rodt, A. Strittmatter, T. Heindel, and S. Reitzenstein, *Rev. Sci. Instrum.* **86**, 013113 (2015).
- [33] J. Bylander, I. Robert-Philip, and I. Abram, *Eur. Phys. J. D* **22**, 295 (2003).
- [34] S. A. Empedocles and M. G. Bawendi, *Science* **278**, 2114 (1997).
- [35] H. D. Robinson and B. B. Goldberg, *Phys. Rev. B* **61**, R5086 (2000).
- [36] V. Türck, S. Rodt, O. Stier, R. Heitz, R. Engelhardt, U. W. Pohl, D. Bimberg, and R. Steingrüber, *Phys. Rev. B* **61**, 9944 (2000).
- [37] G. Sallen, A. Tribu, T. Aichele, R. André, L. Besombes, C. Bougerol, M. Richard, S. Tatarenko, K. Kheng, and J.-P. Poizat, *Nat. Photonics* **4**, 696 (2010).
- [38] J. Houel, A. V. Kuhlmann, L. Greuter, F. Xue, M. Poggio, B. D. Gerardot, P. A. Dalgarno, A. Badolato, P. M. Petroff, A. Ludwig, D. Reuter, A. D. Wieck, and R. J. Warburton, *Phys. Rev. Lett.* **108**, 107401 (2012).
- [39] M. Müller, S. Bounouar, K. D. Jöns, M. Gläßl, and P. Michler, *Nat. Photonics* **8**, 224 (2014).
- [40] Y. M. Galperin, B. L. Altshuler, J. Bergli, and D. V. Shantsev, *Phys. Rev. Lett.* **96**, 097009 (2006).
- [41] C. Gardiner and P. Zoller, *Quantum Noise: A Handbook of Markovian and Non-Markovian Quantum Stochastic Methods with Applications to Quantum Optics*, Springer Series in Synergetics (Springer, New York, 2004).
- [42] B. D. Laikhtman, *Phys. Rev. B* **31**, 490 (1985).
- [43] J. H. Eberly, K. Wódkiewicz, and B. W. Shore, *Phys. Rev. A* **30**, 2381 (1984).
- [44] H. Carmichael, *Statistical Methods in Quantum Optics I—Master Equation and Fokker-Planck Equations* (Springer, New York, 1999).
- [45] R. B. Patel, A. J. Bennett, I. Farrer, C. A. Nicoll, D. A. Ritchie, and A. J. Shields, *Nat. Photonics* **4**, 632 (2010).
- [46] E. B. Flagg, A. Muller, S. V. Polyakov, A. Ling, A. Migdall, and G. S. Solomon, *Phys. Rev. Lett.* **104**, 137401 (2010).
- [47] H. Bernien, L. Childress, L. Robledo, M. Markham, D. Twitchen, and R. Hanson, *Phys. Rev. Lett.* **108**, 043604 (2012).
- [48] X.-s. Ma, S. Zotter, J. Kofler, T. Jennewein, and A. Zeilinger, *Phys. Rev. A* **83**, 043814 (2011).